Mainstream partial nitritation/anammox with integrated fixed-film activated sludge : combined aeration and floc retention time control strategies limit nitrate production

Reference:
Seuntjens Dries, Carvajal Arroyo Jose M., Van Tendeloo Michiel, Chatzigiannidou Ioanna, Molina Janet, Nop Samnang, Boon Nico, Vlaeminck Siegfried.- Mainstream partial nitritation/anammox with integrated fixed-film activated sludge : combined aeration and floc retention time control strategies limit nitrate production
Bioresource technology - ISSN 0960-8524 - 314(2020), 123711
Full text (Publisher's DOI): https://doi.org/10.1016/J.BIORTECH.2020.123711
To cite this reference: https://hdl.handle.net/10067/1700540151162165141

Journal Pre-proofs

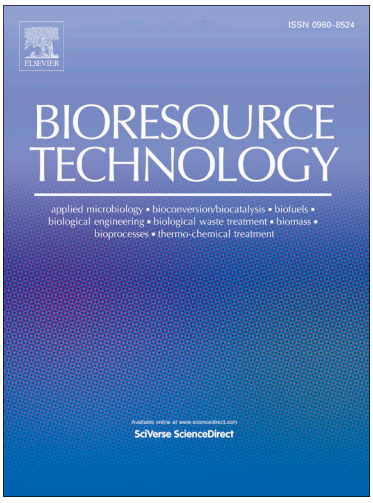

Mainstream partial nitritation/anammox with integrated fixed-film activated sludge: Combined aeration and floc retention time control strategies limit nitrate production

Dries Seuntjens, Jose M. Carvajal Arroyo, Michiel Van Tendeloo, Ioanna Chatzigiannidou, Janet Molina, Samnang Nop, Nico Boon, Siegfried E. Vlaeminck

PII: S0960-8524(20)30983-4
DOI: https://doi.org/10.1016/j.biortech.2020.123711
Reference: BITE 123711

To appear in: *Bioresource Technology*

Received Date: 4 May 2020
Revised Date: 16 June 2020
Accepted Date: 17 June 2020

Please cite this article as: Seuntjens, D., Arroyo, M.C., Van Tendeloo, M., Chatzigiannidou, I., Molina, J., Nop, S., Boon, N., Vlaeminck, S.E., Mainstream partial nitritation/anammox with integrated fixed-film activated sludge: Combined aeration and floc retention time control strategies limit nitrate production, *Bioresource Technology* (2020), doi: https://doi.org/10.1016/j.biortech.2020.123711

Mainstream partial nitritation/anammox with integrated fixed-film activated sludge: Combined aeration and floc retention time control strategies limit nitrate production

Dries Seuntjens[a], Jose M. Carvajal Arroyo[a], Michiel Van Tendeloo[b], Ioanna Chatzigiannidou[a], Janet Molina[a], Samnang Nop[c], Nico Boon[a], Siegfried E. Vlaeminck[b,*]

[a] CMET - Center for Microbial Ecology and Technology, Ghent University, Coupure Links 653, 9000 Gent, Belgium

[b] Research Group of Sustainable Energy, Air and Water Technology, University of Antwerp, Groenenborgerlaan 171, 2020 Antwerpen, Belgium

[c] Imec, ELIS - IDLab, Ghent University, Belgium

[*]Corresponding author. Phone: +3232653689; E-mail: siegfried.vlaeminck@uantwerpen.be

Abstract

Implementation of mainstream partial nitritation/anammox (PN/A) can lead to more sustainable and cost-effective sewage treatment. For mainstream PN/A reactor, an integrated fixed-film activated sludge (IFAS) was operated (26°C). The effects of floccular aerobic sludge retention time ($AerSRT_{floc}$), a novel aeration strategy, and N-loading rate were tested to optimize the operational strategy. The best performance was observed with a low, but sufficient $AerSRT_{floc}$ (~7d) and continuous aeration with two alternating dissolved oxygen setpoints: 10 minutes at 0.07-0.13 mg O_2 L^{-1} and 5 minutes at 0.27-0.43 mg O_2 L^{-1}. Nitrogen removal rates were 122±23 mg N L^{-1} d^{-1}, and removal efficiencies 73±13%. These conditions enabled flocs to act as nitrite sources while the carriers were nitrite sinks, with

low abundance of nitrite oxidizing bacteria. The operational strategies in the source-sink framework can serve as a guideline for successful operation of mainstream PN/A reactors.

Keywords: Deammonification; Nitrification; Nitrosomonas; Nitrospira; Brocadia

1 Introduction

Partial nitritation/anammox (PN/A) is a well-known and widely applied technology for treatment of high-strength ammonium wastewaters (N = 500-1000 mg N L^{-1}) at elevated temperatures (>25°C), for example in the side stream (sludge line) of a sewage treatment plant (STP) (Lackner et al., 2014). Application of the technology in the main stream (water line), combined with a first C-stage that redirects incoming organic carbon towards a digester to produce biogas, can theoretically yield energy-positive STP. PN/A depends on the teamwork of aerobic and anoxic ammonium-oxidizing bacteria (AerAOB and AnAOB), who convert the incoming ammonium to nitrogen gas. To achieve high N-removal efficiencies, suppression of nitrite oxidizing bacteria (NOB), competing with AnAOB for nitrite, is necessary. This suppression remains the main challenge for the application of the technology on pretreated sewage or mainstream PN/A (Agrawal et al., 2018).

Literature proposes a myriad of strategies on how to suppress NOB in mainstream PN/A (Agrawal et al., 2018). Recent advances included more complex reactor operation in so-called hybrid reactor technologies where flocs with high aerobic activity coexist together with biofilms, *i.e.* on a carrier or in a granule, that hosts both aerobic and anoxic microbial conversions. This type of configuration aims to overcome the aerobic rate limitations found in biofilm-only technologies, like granular or membrane moving bed biofilm reactors (MBBR) (Agrawal et al., 2018). Furthermore, to successfully operate hybrid reactors kinetic,

suppression/stimulation or ON/OFF control, *i.e.* by aeration strategy or residual ammonium concentrations, can be coupled with IN/OUT control. By selection on size (sieves) or density (hydrocyclones or external settlers), the floccular sludge retention time (SRT) can be uncoupled from the biofilm SRT. This enables high retention of the slow growing AnAOB and a shorter floccular SRT to achieve sufficient AerAOB activity, yet gradual wash-out of NOB when the right process conditions are given. This IN/OUT control is most easily controlled in integrated fixed-film activated sludge (IFAS) reactors, where biofilm on carriers and flocs can be more easily separated than a granule-floc sludge matrix. Therefore, this reactor type is highly suitable for better understanding of the complex web of interactions which constitutes mainstream PN/A.

The few studies published on hybrid PN/A technologies on pretreated sewage showed promising results, with low nitrate production over ammonium conversion ratios in a range of 4-30% at 16-30°C (Han et al., 2016; Laureni et al., 2016; Malovanyy et al., 2015; Yang et al., 2017; Laureni et al., 2019; Pedrouso et al., 2019). Overall, the studies utilized residual ammonium concentrations >2 mg NH_4^+-N L^{-1} to maximize AerAOB and AnAOB activity. Other operational strategies were however different. Laureni et al (2016) and Yang et al (2017) reported continuous aeration at a low DO setpoint (<0.2 mg O_2 L^{-1}), combined with either short (7d) or high floccular SRT (40d) at 22-25°C. Han et al. (2016) and Pedrouso et al. (2019) used intermittent aeration at a high DO setpoint of 1.5 mg O_2 L^{-1}, combined with either a very short aerobic floccular SRT ($AerSRT_{floc}$) of 2.8d at 30°C or an uncontrolled SRT at 15-21°C. Since a wide and sometimes contrasting range of SRT values (i.e. 7 vs. 40d), aeration pattern (continuous vs. intermittent) and DO setpoints (<0.2 vs. 1.5 mg O2 L^{-1})

were applied in previous studies, the interaction between and combination of $AerSRT_{floc}$ and the aeration regime needs further attention.

In this study, an IFAS reactor treated synthetic pretreated sewage at 26-27°C for a period of almost a year. The reactor was operated as sequencing batch to mimic substrate gradients experienced in full-scale plug-flow conditions, ensuring residual ammonium concentrations during process operation to enhance AerAOB and AnAOB activity (Third et al., 2001). Different $AerSRT_{floc}$ in combination with different innovative aeration strategies (DO setpoints and aeration patterns) were tested to unravel the factors governing the AnAOB, AerAOB and NOB activity distribution over carrier and floc. The final goal was to obtain predictable operational strategies to maximize NOB suppression.

2 Material and Methods

2.1 Reactor operation

2.1.1 Reactor set-up

An SBR with 4.5L working volume (33% volume exchange ratio) was operated for almost a year at 26-27°C. The dissolved oxygen (DO) setpoint was controlled by a Hach Lange LDO sc probe and SC100 controller. The airflow rate was manually adjusted by an airflow regulator (OMA-1, Dwyer, Indiana, US) in a range of 0.1-1 L $min.^{-1}$. The pH was controlled at 7.2 using the same controller by dosage of 0.05 M NaOH. DO and pH values were logged by a LabJack data-acquisition card and Daqfactory software (Azeotech, Oregon, US). A reactor cycle consisted of the following steps: 1) 45 min. of feeding and aerobic reaction time, 2) 12-140 min. of aerobic reaction time, depending on the loading rate of the reactor, 3) 4 min. of non-aerated mixing, 4) 20 min. settling time, 5) 4 min. of liquid withdrawal.

78 **2.1.2 Sludge seeding**

79 Carriers were seeded (30% filling ratio) from Anoxkaldness K1 carriers grown for over 1
80 year in an oxygen limited (without aeration) moving bed biofilm reactor (MBBR) for AnAOB
81 enrichment under mainstream conditions (influent 50 mg $NH_4^{\pm}N$/ 50 mg NO_2-N L^{-1}).
82 Floccular sludge from an industrial partial nitritation (NAS®) reactor was seeded four times
83 over the experiment (**Figure 1, black arrows**).

84 **2.1.3 Influent**

85 Before the reported operational periods, the reactor was operated for 59 days under a
86 completely autotrophic IFAS mode. During the operational periods, the reactor was fed
87 with a synthetic influent mimicking sewage after primary treatment. Tap water at 26-27°C
88 was mixed with a concentrated feed stored at 4°C that includes NH_4Cl, KH_2PO_4, $NaHCO_3$,
89 and trace elements. The final concentrations in the influent were 40-50 mg NH_4^+-N L^{-1},
90 1.8±1.4 mg NO_3^--N L^{-1}, 0.48±0.47 mg NO_2^--N L^{-1}, ~0.5 g $NaHCO_3$ L^{-1}, 5 mg PO_4^{3-}-P L^{-1}, and 1
91 mL L^{-1} trace element solutions A and B (according to van de Graaf et al., 1996).
92 Biodegradable COD (bCOD) was added to promote floc growth, and for the bCOD/N range
93 of 0.5-1, a concentrated, cold stored (4°C) glucose solution was added in a pulse wise
94 manner during feeding. To further promote floc growth, bCOD/N was increased to a level
95 of 2 at day 257. The bCOD source from day 257 onwards consisted of a mixture of acetate
96 (20%), starch (65%) and yeast extract (15%, about 1 mg N L^{-1}) to mimic the more slowly
97 biodegradable nature of bCOD in pretreated sewage. This composition was in line with
98 previously reported studies using real wastewater, with a reported average TN

99 concentration of 43-45 mg TN L^{-1} and bCOD/N ratio of 1.8-2.5 (Malovanyy et al., 2015 and
100 Pedrouso et al., 2019).

101 **2.1.4 Sampling**

102 Influent and effluent samples were taken regularly and filtered over a 0.2 µm filter, prior to
103 storage (4°C) and analysis of nitrogen species. Total and volatile suspended solids (TSS and
104 VSS) were measured of the mixed liquor together with the over 24h collected effluent
105 samples to calculate the $AerSRT_{floc}$. Biofilm sludge content was not measured. Carriers and
106 flocs were sampled for molecular analysis. Carriers were immediately stored at -20°C, and
107 flocs from the mixed liquor were pelletized by centrifugation for 10 min at 20,817 relative
108 centrifugal force (RCF) and stored at -80°C.

109 ## 2.2 Batch activity tests

110 Five batch activity tests (**Figure 1, red arrows**) were executed to determine AerAOB, AnAOB
111 and NOB *ex-situ* potential activities, further referred to as rAerAOB, rAnAOB and rNOB.
112 Flocs and carriers (5 randomly taken from the reactor per test) were brought separately in
113 a pH 7.2 corrected medium with 3.87 g HEPES L^{-1}, 0.2 g $CaCl_2 \bullet 2H_2O$ L^{-1}, 0.1 g $MgSO_4 \bullet 7H_2O$
114 L^{-1}, 5 mg $Na_2HPO_4 \bullet 2H_2O$-P L^{-1}, 0.5 g $NaHCO_3$ L^{-1}, and 1mL L^{-1} trace elements A and B. Anoxic
115 tests were run in penicillin bottles flushed with N_2 gas. Spikes of 50 mg NH_4Cl-N and 25 or
116 50 mg $NaNO_2$-N L^{-1} were given at the beginning of the aerobic and anoxic test, respectively.
117 Concentrations of NO_2^-, NO_3^- and NH_4^+ were determined over time. Protein measurements
118 were done to quantify floccular sludge concentration for the calculation of biomass specific
119 rates (mg N g $biomass^{-1}$ protein d^{-1}). For the carriers, activities were calculated
120 volumetrically (per 5 carriers). All tests were performed in triplicate.

121 ## 2.3 Physicochemical analyses

122 NO_2^--N and NO_3^--N were measured with a 761 Compact IC (Metrohm, CH). NH_4^+ was
123 measured with the Nesslerization method, while volatile suspended solids (VSS) and total
124 suspended solids (TSS) were measured per Standard Methods 2540D and E (Greenberg et
125 al., 1995). Protein concentrations were determined using Lowry method, with bovine
126 serum albumin as a standard (Lowry et al., 1951). The sludge was washed twice prior to
127 analysis to prevent interference by the HEPES buffer.

128 ## 2.4 Calculations of distributions between carrier and floc

129 The distribution of AnAOB, AerAOB and NOB activity between floc or the biofilm on the
130 carrier was calculated by fitting the batch test activity data to the reactor performance
131 data. First, the potential activity by floc and carrier in the reactor was estimated by
132 extrapolation of the potential activities measured in the batch tests. The extrapolation was
133 calculated with the floccular sludge concentration (with g VSS reactor, and ratio g protein/
134 g VSS = 0.8) and number of carriers in the reactor (=1390). The potential activities were
135 then corrected with the aerated fraction during that operational phase for AnAOB, AerAOB,
136 and NOB, since it was assumed that AnAOB, AerAOB and NOB main activity was during this
137 period (not during settling/anoxic mixing). The potential activity was then corrected with
138 the average oxygen concentration by means of a Monod saturation model (for AerAOB,
139 NOB), while nitrogen limitations were assumed to have no effect on the activity. This is for
140 nitrite due to the low substrate affinities for NOB *Nitrospira* and AnAOB *Brocadia*, and for
141 ammonium due to SBR cycling with only short periods of low ammonium concentrations.
142 To account for the different diffusional limitations in biofilm and floc, a biofilm over floc

143 saturation factor (>1) was introduced. The NOB oxygen affinity constant $KO_{2,NOB}$ was taken
144 as literature value, being 0.23 mg O_2 L^{-1}, since no significant differences are reported for
145 different *Nitrospira* species (Ushiki et al., 2017). The AerAOB oxygen affinity constant
146 ($KO_{2,AOB}$) and biofilm over floc saturation factor were then fitted to the data until the
147 calculated nitrogen balance fitted the measured N-balance (in %) during operation, by
148 minimizing the average residuals over the selected period. The fitted $KO_{2,AerAOB}$ was 0.32 mg
149 O_2 L^{-1}, with a biofilm over floc saturation factor of 1.78. The average error between the
150 model and measured activities for AnAOB, AerAOB and NOB was 11±8%, 10±10%, and
151 3±1.5% respectively.

152 **2.5 Estimation of biofilm surface area**

153 A pixel-based image-recognition methodology estimated the surface area of the biofilm.
154 Pictures of carriers were taken with a Canon EOS 700D (T2 / canon AF T2-T2 1,6x SLR
155 426115) mounted on an Olympus SZH-ILLK stereomicroscope under identical lightning
156 conditions. The surface area of the biofilm was estimated by analyzing the images. The
157 main rationale was that the biofilm can be distinguished by the red-brownish color. The
158 photo-background and carrier were colored as black and white respectively. Firstly, the
159 contrast and brightness of the images was increased by equalizing each channel of the
160 histogram. Secondly, brown colors in the biofilm (RGB range from 190-0-0 to 255-50-50)
161 were converted to red color (RGB-value 255-0-0). The same technique was used to identify
162 the background and the holder into a uniform white and light blue color. Finally, the
163 number of pixels needed to fit 1 mm^2 was calculated using the image of a ruler. The surface
164 area of the biofilm was then calculated with the following formula:

165 $$Biofilm\ surface\ area = \frac{\sum red\ pixels\ (RGB = 255 - 0 - 0)}{46010\ \frac{pixels}{mm^2}}$$ The carrier filling ratio (%)

166 for each quarter of the K1-carrier was calculated as the normalization of the biofilm surface

167 area over the surface area of the quarter.

168 The biofilm thickness was estimated by dividing the surface area over the perimeter of one

169 quarter, being 16 mm, for the thin biofilms, and a smaller perimeter of 10 mm for the thick

170 biofilms, due to the triangular shape of the quarter.

171 **2.6 Molecular analysis**

172 Over the operational period, samples of flocs and carriers were taken in triplicate, except

173 for day 12 (3x floc, 1x carrier), day 148 (3x floc, 2x carrier), day 197 (2x floc, 3x carriers), day

174 213 (3x floc, 0x carrier), and day 325 (0x floc, 10x carrier: 5x thick and 5x thin). Floc

175 samples were taken from the reactor at maximum reactor volume (4.5 L), pelletized and

176 stored at -80°C. Carriers with the biofilm were taken randomly and stored at -20°C. Before

177 extraction, the carriers were added in 1.5 mL sterile phosphate buffered saline (PBS tablets,

178 Sigma Aldrich, Belgium) and sonicated twice for 15 min to remove the total biofilm from

179 the carrier. The biofilm diluted in PBS was then transferred to a 1.5 mL DNA extraction tube

180 and pelletized.

181 Details on the DNA extraction, quality validation, sequencing and data processing can be

182 found in Seuntjens et al. (2018b). In brief: the V3-V4 region was sequenced with Illumina

183 MiSeq, processed with MOTHUR software, aligned to the SILVA v123 database, tidied up

184 and clustered in OTUs with 97% similarity, and classified using the MIDAS database.

185 The reads from 16S rRNA gene amplicon sequencing were imported in R (v3.3.2).
186 Singletons, OTUs with no more than one read in every sample, were removed (McMurdie,
187 2014). α-diversity was calculated based on the Hill numbers, adjusting the diversity
188 command of the PhenoFlow package (v1.0) (Props, 2016) in R. β-diversity NMDS graphs
189 were generated based on Jaccard dissimilarity index. The phyloseq package (McMurdie,
190 2014) in R (v3.3.2) was used to generate the plots representing the ten most relative or
191 absolute abundant genera. The replicates were merged using the 'merge_samples'
192 command of the phyloseq package. Finally, the differential abundance of OTUs in samples
193 were calculated using the DESeq2 package (v1.16.1), converting the phyloseq object with
194 the command 'phyloseq_to_deseq2' from the phyloseq package in R (v3.3.2). The
195 Benjamini-Hochberg multiple-inference correction was used and significantly enriched
196 OTUs were considered the ones with two-fold change >-2 or <2 and corrected p-value
197 <0.01.

198 # 3 Results & Discussion

199 ## 3.1 Overall experiment and performance

200 The results of the experiment are given in **Figure 1** and stable operational periods are
201 summarized in **Table 1**. The main variables that were changed were the aerobic floccular
202 sludge retention time ($AerSRT_{floc}$) and continuous aeration strategy (one-point and two-
203 point aeration), while the N loading rate and influent bCOD/N ratio were occasionally
204 changed. Industrial PN sludge was occasionally seeded (**Figure 1, black arrows**) at the start
205 of an operational strategy with high $AerSRT_{floc}$ (Phase I and VIa) to obtain sufficient
206 floccular biomass.

The tested operational conditions during Phases I-V failed to establish a decent performance and are later discussed in more detail. The combination of a low DO setpoint (0.06-0.15 mg O_2 L^{-1}) with low $AerSRT_{floc}$ (Phase II-IV) did not result in sufficient AerAOB activity in the reactor and a low DO setpoint (0.15 mg O_2 L^{-1}) with high $AerSRT_{floc}$ (Phase I) did result in good AerAOB activity but low N removal. From Phase V onwards, two-point aeration was used to obtain higher AerAOB activity and excess nitrite production at high DO setpoint (initially based on $KO_{2,AerAOB}$ = 0.32 mg O_2 L^{-1}) in combination with AnAOB consuming the accumulated nitrite at low DO setpoint. Additionally, the nitratational lag in NOB is exploited by frequently switching from aerobic to local anoxic conditions (Agrawal et al., 2018). The best performance of the reactor was achieved in Phase VIa, with two-point aeration and a sufficient $AerSRT_{floc}$ of 6.8±3 d, in contrary to Phase V where a low $AerSRT_{floc}$ of 4.1 d and a low N loading rate failed to achieve sufficient N removal. The addition of floccular sludge at the start of Phase VIa resulted in an immediate but short (<3 d) increase in N removal efficiency, since this type of seeding did not allow for successful AerAOB bio-augmentation as stated in Section 3.4. Consequently, the continuous increase in efficiency over the following weeks was more likely caused by the improved operational conditions. In the early stage of Phase VIb, a similar performance as in Phase VIa was reached. The application of a higher $AerSRT_{floc}$ at the end of phase VIb resulted in an increased nitrate production ratio. The contribution of influent bCOD to the overall N removal was neglectable since almost all bCOD was removed aerobically, as discussed in section 3.5, and a low influent bCOD/N of 0.25-1.0 was used in Phase I-VIa.

228 Phase VIa achieved a nitrogen removal rate of 122±23 mg N L^{-1} d^{-1} with a nitrate production
229 ratio of 18±6% over a stable period of 18 d, corresponding to roughly three SRT_{floc}. Similar
230 results under similar conditions were obtained during the early stage of Phase VIb over 29
231 d. The main differences were a higher influent COD/N ratio, which was later proved to have
232 a neglectable influent on the N removal, and a higher N loading rate and thus a shorter
233 aerobic reaction phase. Future studies should confirm these findings under longer term
234 steady state conditions. The reported N removal rate is slightly higher than other hybrid
235 reactor systems at temperatures of 25-31°C, with rates of 97-100 mg N L^{-1} d^{-1} and low
236 nitrate production ratios of 4-19% (Yang et al., 2017; Han et al., 2016). Two other IFAS
237 studies at 25°C showed similar nitrate production ratios, yet with lower N removal rates of
238 47-55 mg N L^{-1} d^{-1} (Laureni et al., 2016; Malovanyy et al., 2015). Some biofilm-only single-
239 stage PN/A at ~25°C reported similar removal efficiencies (>77%), but lower removal rates
240 (10-47 mg N L^{-1} d^{-1}), mainly due to aerobic diffusional limitations (Gilbert et al., 2014;
241 Laureni et al., 2016). Other single stage PN/A or nitritation/denitritation systems at 25°C
242 reported higher removal rates (150-500 mg N L^{-1} d^{-1}), yet with lower N removal efficiencies
243 (35-66%), mainly due to residual ammonium levels or higher nitrate production (De
244 Clippeleir et al., 2013; Lotti et al., 2008; Regmi et al., 2014). At a lower temperature of 15°C,
245 two IFAS studies achieved high N removal efficiencies of 72-88%, but with lower volumetric
246 removal rates of 39-79 mg N L^{-1} d^{-1} (Pedrouso et al., 2019; Laureni et al., 2019).
247 Furthermore, the obtained N removal rate is comparable with those achieved in
248 conventional activated sludge systems based on nitrification/denitrification (100-150 mg N^{-}
249 ^{1} L^{-1} d^{-1}) (Wiesmann, 1994). This shows the feasibility of mainstream PN/A in countries with

250 sewage temperatures over 25°C, influent ammonium concentrations up to 45-50 mg N L^{-1},
251 with discharge limits of 10-15 mg TN L^{-1} as similar effluent concentrations were achieved
252 during Phase VIa. A final effluent polishing step (e.g. similar to Le et al., 2019) or a better
253 utilisation of influent bCOD (e.g. application of a pre-denitrification tank) could further
254 improve the performance.

255 3.2 Mapping the microbial balance in IFAS PN/A

256 The potential activity of AnAOB, AerAOB and NOB in the floccular biomass and carriers
257 were separately evaluated by performing *ex-situ* batch tests after different periods under
258 stable operational conditions (**Figure 1, red arrows**). These batch activities were then
259 compared to the performance of the reactor under each specific set of conditions (**Figure**
260 **2**). High $AerSRT_{floc}$ (26 d) and one-point aeration (0.15 mg O_2 L^{-1}) allowed excessive NOB
261 growth (Phase I) and caused the highest NOB activity in both carriers and flocs ($rmax_{NOB.floc}$
262 = 469 mg N g $protein^{-1}$ d^{-1}, rAerAOB/rNOB = 1.4). One-point aeration (0.15 mg O_2 L^{-1}) and a
263 $AerSRT_{floc}$ as low as 4.1d, during phase IV, enabled for superior NOB suppression
264 ($rmax_{NOB.floc}$ = 115 mg N g $protein^{-1}$ d^{-1}, rAerAOB/rNOB = 6) but did not support AerAOB
265 growth and high ammonium levels remained in the effluent with no nitrite accumulated.
266 Finally, during Phase VIa, two-point aeration and sufficient AerSRT of 6.8d supported
267 AerAOB activity while promoting further wash-out of NOB in the floc fraction ($rmax_{NOB.floc}$ =
268 32 mg N g $protein^{-1}$ d^{-1}, rAerAOB/rNOB = 29). Additionally, the highest AnAOB activity in the
269 reactor was observed during this phase, removing on average 84% of the produced nitrite
270 by AerAOB (**Figure 2**). The contribution of bCOD on N removal can be neglected (Section
271 3.5). The high contribution of AnAOB activity was confirmed by the rapidly increasing

272 relative abundance of *Ca. Brocadia* from Phase V to the end of Phase VIb (**Figure 3**).
273 Overall, the reactor nitrate production ratio was inversely correlated to the proportional
274 anammox capacity on the carrier (rAnAOB/rNOB) when $AerSRT_{floc}$ varied from 4.1-7.7 d
275 (**Figure 4**). Besides the inverse correlation, the highest rAnAOB/rNOB in the carriers (1.5)
276 was only achieved with two-point aeration and short $AerSRT_{floc}$, which enabled the flocs to
277 supply nitrite for the carriers.
278 A balanced hybrid PN/A can thus be achieved when the flocs act as a nitrite source while
279 nitrite scavenging that controls nitrate production is forced to occur in the biofilm, which is
280 comparable to sidestream hybrid PN/A (Hubaux et al., 2015). Laureni et al. (2019) identified
281 with a model that the presence of AnAOB activity in the biofilm, acting as NO_2^- sink, was the
282 key mechanism for NOB suppression in flocs. This was further supported by the molecular
283 analysis on the autotrophic N-community (AnAOB, AerAOB, NOB) where most AnAOB
284 (*Brocadia*) were preferentially enriched in the carrier, NOB (*Nitrospira*) enrichment lingered
285 slightly more in the floc than in the carrier and one of the most dominant AerAOB
286 (*Nitrosomonas* OTU 143) was preferentially enriched in the floc. This OTU was also most
287 abundant in the floc in the most performant Phase VIa. Therefore, in the next sections, we
288 discuss different control mechanisms to stimulate and retain AerAOB as floccular nitrite
289 source and stimulate AnAOB/suppress NOB in the carrier nitrite sink. This discussion
290 interlinks the information obtained from the operational parameters (**Figure 1**), batch-
291 activity tests (**Figure 2**) and microbial community analysis (**Figure 3**).

292 ## 3.3 The floc as nitrite producer

293 **Low $AerSRT_{floc}$ produced higher potential rAerAOB/rNOB activity ratios in the floc at low**
294 **DO setpoints.** The rAerAOB/rNOB increased from 1.4 to 7.5 when $AerSRT_{floc}$ was lowered
295 from 26 to 5 days (Phase I vs. Phase IV). High $AerSRT_{floc,}$ as in Phase I thus most likely
296 prevented NOB washout, resulting in complete oxidation (80%) of the converted
297 ammonium, even at a DO setpoint as low as 0.15 mg O_2 L^{-1} (**Figure 1 & Figure 2, Phase I**).
298 This is consistent with the observations in the beginning of phase VIa, where nitrate
299 production peaked after an increase in $AerSRT_{floc}$, which was also reflected in the increased
300 relative abundance of *Nitrospira* community (**Figure 3, day 213 vs. day 220**). Furthermore,
301 at the end of the experiment (**Figure 1, phase VIb, red shaded area**), an increase of
302 $AerSRT_{floc}$ from 4-6 days to 7-18 days had an important impact on the NOB activity,
303 resulting in an increased nitrate production ratio from 20% up to 45%. This indicates that
304 under these conditions (26-27°C, two-point aeration), tight $AerSRT_{floc}$ control at around 4-7
305 days is necessary to get sufficient AerAOB activity, while too low or high $AerSRT_{floc}$ would
306 cause washout of AerAOB (Phase II-V) or NOB growth (Phase I), respectively. Controlling
307 $AerSRT_{floc}$ in hybrid PN/A is thus crucial to obtain stable process performance, in
308 combination with continuous aeration using two alternating DO setpoints and a high N
309 loading rate. The final choice of the $AerSRT_{floc}$ will go hand in hand with process conditions
310 that determine AerAOB growth and activity: *e.g.* the applied aeration strategy and
311 temperature of the process.
312 The results from Phase I are in stark contrast with a recent study by Yang et al., (2017)
313 where a stable PN/A on pretreated sewage was achieved for 120 d under similar

conditions; T = 20-25°C, $AerSRT_{floc}$ of 40d, continuous one-point aeration <0.2 mg O_2 L^{-1}, and residual ammonium levels >2 mg NH_4^+-N L^{-1}. Assuming that steady state is achieved after three $AerSRT_{floc}$, this strategy proved to be successful. The inoculum could have played a vital role as the study showed high N removal efficiencies since inoculation. Their inoculum's NOB relative abundance was with 0.01% much lower than the 0.3% in our case. As initial high AnAOB activity might directly channel nitrite away from the bulk, NOB exponential growth in the floc is limited and longer $AerSRT_{floc}$ are needed to enable growth. The batch-test rAerAOB/rNOB ratios in the flocs (**Figure 2**) were higher than previously observed in mainstream hybrid PN/A systems at temperatures of 25-30°C: at low $AerSRT_{floc}$ these reached 4.4-29 compared to literature values of 1-1.6 (Han et al., 2016; Malovanyy et al., 2015; Pedrouso et al., 2019). Whereas the previously described values were obtained with intermittent aeration that alternated high DO setpoints (>1 mg O_2 L^{-1}) with anoxia, the here applied continuous aeration at lower DO setpoints seemed to better outcompete NOB. This is consistent with the results of Laureni et al. (2019), who applied continuous aeration at 0.17 mg O_2 L^{-1}, and where molecular methods showed very low numbers of NOB compared to AerAOB in the flocs at 15°C. In contrast, a mainstream nitritation/denitritation study with intermittent aeration (1.6 mg O_2 L^{-1}) at 25°C reported rAerAOB/rNOB values of 5.5-6 (Regmi et al., 2014). AnAOB have recently been shown to have gradual recovery after oxygen inhibition, with the intermittent aeration pattern potentially decreasing AnAOB activity and thus competition for nitrite (Seuntjens et al., 2018a). The observed difference in NOB suppression might thus indicate that AnAOB are more sensitive to oxygen inhibition than denitrifiers.

336 **The floccular sludge concentration controls the maximum nitrite production rate.** The
337 largest part of the AerAOB activity (61-92%) was always located in the flocs over the course
338 of the experiment (**Figure 2**). This is supported by the observed correlation between the
339 volumetric AerAOB activity with the floc concentration range of 0.05 to ~1 g VSS L^{-1}.
340 Depending on the inoculum timepoint and other operational strategies, the AerAOB
341 reactor activity increased from 20 to 80-120 mg N L^{-1} d^{-1} when the floc concentration
342 increased from 0.05 to ~1 g VSS L^{-1}. Additionally, the potential activity of AerAOB in the
343 carriers decreased over time from 40 mg N L^{-1} d^{-1} to about 25 mg N L^{-1} d^{-1}, even when
344 higher DO-set points (0.31-0.51 mg O_2 L^{-1}) during two-point aeration were applied. As
345 AerAOB activity is mainly located in the floc, sufficient floc concentration is necessary to
346 achieve high turnover rates at low DO concentrations. In contrary to the AerAOB, NOB
347 activity shifted from the flocs to the carriers when low $AerSRT_{floc}$ was applied (**Figure 2**).
348 This is in accordance to Li et al. (2019) who observed a significant increase of granular NOB
349 activity after reducing the floccular SRT to 20 days. The competition for nitrite and oxygen
350 between floccular sludge and biofilm seemed to be impacted by $AerSRT_{floc}$. Additional
351 research is required to determine the exact mechanism to outcompete NOB in granules (Li
352 et al., 2019).
353 **Seeding from an industrial partial nitritation reactor did not allow for successful AerAOB**
354 **bio-augmentation.** Flocculent nitritational sludge from a sidestream process was seeded on
355 day 0, 98 and 213. On two days, day 0 and 213, the major AerAOB OTUs that were present,
356 *i.e.* OTU 119 and OTU 143, were washed out of the reactor (**Figure 3, Panel *Nitrosomonas***
357 **community**). Although functionality was observed, *i.e.* there was sufficient ammonium

358 oxidation in the reactor, the augmented OTUs could not thrive under mainstream
359 conditions. These results indicate that when applying bioaugmentation strategies the right
360 AerAOB species need to be selected to cause a long-lasting effect.

361 3.4 The carrier as nitrite sink

362 **Lower DO setpoints stimulate the maximum rAnAOB/rNOB values.** During continuous
363 one-point aeration, a minor decrease of the DO setpoint from 0.15 to 0.06 mg O_2 L^{-1} caused
364 the rAnAOB/rNOB to increase from 0.61 to 0.93 while all other operational parameters, i.e.
365 $AerSRT_{floc}$, loading rate and influent bCOD/N, were similar **(Figure 2, Phase IIb compared to**
366 **Phase IV)**. As oxygen inhibition has been reported for AnAOB at very low DO setpoints of
367 0.02-0.13 mg O_2 L^{-1}, micro-aerobic conditions at the biofilm-liquid interface most probably
368 steer the competition for nitrite (Dalsgaard et al., 2014). A previous study on large PN/A
369 granules (>500 µm) showed stratification of aerobic (O_2 penetration depth: 100 µm at 0.14
370 mg O_2 L^{-1}) and anoxic processes in the biofilm (Nielsen et al., 2005; Vlaeminck et al., 2010).
371 This indicates that the lower DO set-points most likely created less oxygen penetration in
372 the biofilm and therefore also less space for aerobic processes, increasing the
373 rAnAOB/rNOB. Furthermore, the study found that the hydraulic regime seemed to be
374 crucial in regulating mass transfer in the diffusive boundary layer, where low mixing
375 resulted in a much lower O_2 penetration depth (~50 µm). For IFAS-related applications,
376 oxygen consumption by flocs and carriers, as function of nitrogen and carbon load, as well
377 as reactor turbulence and heterogeneity will influence mass transfer in this diffusive
378 boundary layer, governing competition in the biofilm. Optimization of these parameters
379 may therefore result in higher rAnAOB/rNOB in the carrier.

380 **Higher nitrogen loading rates might increase competition for nitrite and space in the**
381 **biofilm.** Since aerobic activity on the biofilm is limited due to the previous discussed effects
382 of mass transfer, higher loading rates will give rise to more floccular nitrite production per
383 biofilm surface area when the floc acts as a nitrite source. This provides a competitive
384 advantage for AnAOB in the biofilm that might be able to outgrow NOB in the competition
385 for nitrite and space. This hypothesis is supported by the substantial difference in
386 performance of the two two-point aeration phases V and VIa, operated at a loading rate of
387 64 and 153 mg N L^{-1} d^{-1} respectively. When shifting from phase V to VIa, the potential
388 activity of AerAOB and NOB on the carrier decreased similarly, from ~30 towards ~25 mg N
389 L^{-1} d^{-1}. In contrast, the potential activity of AnAOB increased, with a rAnAOB/rNOB increase
390 from 0.46 to 1.47. This resulted in the best reactor performance with a decrease in nitrate
391 production ratio of 44 to 18%. The activity results were not reflected by similar shifts in
392 relative abundance of AnAOB and NOB on the carrier (**Figure 3, Panel 3 on AnAOB, AerAOB**
393 **and NOB community**). The AnAOB/NOB abundance ratio did not show a clear increase, but
394 a slight decrease from 7 to 5. The following explanation might explain the discrepancy: 1)
395 heterogeneity of sampling (mainly thick biofilms were sampled), 2) inherent variations from
396 each analysis step (DNA extraction, PCR, etc.), 3) deeper changes in microbial community
397 structure (e.g. NOB *Nitrospira* sublineage II to I), and 4) longer biofilm sludge retention
398 times, where inactive or dead AnAOB/NOB biomass might not reflect actual activity.
399 **Biofilm thickness did not impact the microbial abundance in the carriers.** At the end of the
400 experiment (day 325), different carriers were sampled in the reactor and classified as thick
401 biofilms (avg. biofilm thickness = 1.1 ± 0.1 mm) and thin biofilms (avg. biofilm thickness =

402 0.3 ± 0.2 mm). The community analysis did not reveal any significantly different OTUs
403 between the thick and thin biofilms, both for the autotrophic nitrogen community as for
404 the 15 most abundant members of the so-called satellite community. The thin biofilms
405 however had a higher, although not significantly, different AnAOB/NOB relative abundance
406 ratio of 9.4±5.1 vs. 5.9±2.2 compared to the thick biofilms. Furthermore, from the
407 randomly sampled carriers over the course of the experiment, which classified mostly as
408 thick carriers, the thick and thin biofilms did not differ, confirming the results of the last day
409 sampling campaign. The results are not in line with the current understanding of thick and
410 thin biofilms in sidestream PN/A. There, larger biofilm thicknesses and granule diameters 1-
411 2 mm vs. 0.1-0.2 mm had higher AnAOB enrichment, resulting in higher AnAOB/NOB ratios,
412 providing better suppression of NOB (Nielsen et al., 2005; Vlaeminck et al., 2010). One
413 explanation might be that diffusional limitations, namely low nitrite levels in the bulk (<1
414 mg N L^{-1}) could have limited AnAOB growth in the inner part of the thick biofilms.
415 Furthermore, the very low applied oxygen levels (~0.05 mg O_2 L^{-1}) could have limited
416 aerobic growth in the thin biofilms as previously described. From our results, at the level of
417 AnAOB and NOB abundance, and within a biofilm thickness range of 0.08 to ~2.5 mm, it
418 seems that biofilm thickness will not be a major factor controlling the rAnAOB/rNOB ratio.
419 Yet, further confirmation of actual activity is necessary since NOB abundance does not
420 always reflect their activity in these biofilms (Winkler et al., 2012).

421 ## 3.5 The impact of biodegradable organic carbon

422 **Influent biodegradable organic carbon (bCOD) was almost completely oxidized while**
423 **partial denitrification can increase nitrogen removal.** To assess the fate of bCOD, a reactor

424 cycle at day 288 was monitored. Two 15 mg bCOD L^{-1} spikes were added after feeding
425 (**Figure 5**). The spikes were given during a low (0.05 mg O_2 L^{-1}) and high (0.3 mg O_2 L^{-1}) DO
426 setpoint on minutes 15 and 40, respectively. Overall, from the mass balance, 80% of the
427 bCOD was removed aerobically at the low DO setpoint while at the high DO setpoint all
428 bCOD was lost aerobically. These results match the ones from Laureni et al. (2016), where
429 at a DO setpoint of 0.1-0.2 mg O_2 L^{-1} almost all bCOD was lost aerobically. Consequently,
430 the influence of influent bCOD on N removal can therefore be neglected since most bCOD
431 (80-100%) was removed aerobically and influent bCOD/N ratios were low (0.25-1.0 for
432 Phase I-VIa and 2.0 for Phase VIb).
433 Interestingly, with the bCOD spike at the low DO setpoint (~0.05 mg O_2 L^{-1}), nitrate
434 concentrations decreased during the next ten minutes in the reactor in concomitance with
435 nitrite accumulation, indicating that some partial denitrification might take place next to
436 full denitrification. Engaging this pathway in PN/A would allow nitrite production and
437 increase in N removal performance. Partial denitrification has been reported in PN/A
438 reactors and it is suggested that low influent bCOD/N ~ <2.6 concentrations, easy
439 biodegradable bCOD (*e.g.* acetate), residual nitrate (>2 mg N/L) or cross-feeding promote
440 the pathway (Du et al., 2016; Malovanyy et al., 2015; Le et al., 2019; Speth et al., 2016).
441 From the sequencing analysis, seven of the 15 most abundant OTUs are known to
442 potentially express nitrate reductase and found in (partial) denitrifying environments:
443 genus *Thauera* (phylum β-proteobacteria) (Du et al., 2016), genus *WCHB1-50* (Chloroflexi)
444 (Speth et al., 2016), genus *Ignavibacterium* (Chlorobi) and *K2-30-37* (Chlorobi) (Agrawal et

445 al., 2017), genus *Brevundimonas* (α-proteobacteria) (Srinandan et al., 2011), and genus
446 *Blastocatella* (Acidobacteria) (Speth et al., 2016) .
447 The bCOD change mainly stimulated the growth of the genus *Thauera*, which preferentially
448 grew in the floc (2 → 22% relative abundance). *Thauera sp.* were earlier associated with
449 partial denitrification, with acetate as bCOD source (Du et al., 2016). As the new bCOD
450 mixture also contained acetate, these bacteria might also have used this to partially
451 denitrify. In the carrier, the phyla Chloroflexi (6.6%) and Chloribi (~8.2%) were dominant
452 with the genus *Ignavibacterium* (Chloribi) increasing in relative abundance with the new
453 bCOD mixture. These phyla (and other core phyla in the reactor *i.e.* Bacteroidetes;
454 Sphingobacteriaceae) are commonly associated with more autotrophic PN/A systems,
455 potentially forming a core microbiome of PN/A reactors (Lawson et al., 2017). It is
456 suggested that they potentially thrive through internal carbon recycling, *i.e.* degeneration
457 of extracellular peptides while reducing nitrate to nitrite to fuel anammox (Agrawal et al.,
458 2017; Lawson et al., 2017; Speth et al., 2016).
459 **The bCOD mixture of acetate, yeast extract and starch increased the autotrophic**
460 **community's relative abundance.** On day 256, the bCOD (~40 mg bCOD L^{-1}) was changed
461 from glucose to the above described mixture (~80 mg bCOD L^{-1}) to enhance floc formation
462 and growth. Instead of stimulating the growth of heterotrophs, the increase in bCOD
463 caused the autotrophic N-community relative abundance to almost triple in both flocs and
464 carriers (**Figure 3, Panel 3, day 256 vs. 312**). From reactor operation, no clear changes
465 could have influenced this change as the floc concentration stabilized around ~0.5 g VSS L^{-1}
466 (**Figure 1, Panel A**) and $AerSRT_{floc}$ remained constant (**Figure 1, panel A**), while the AnAOB,

467 AerAOB and NOB volumetric activities remained constant. AnAOB and NOB showed the
468 strongest increase in relative abundance. For some *Brocadia* species it is known that they
469 can use acetate as electron donor to reduce nitrate, which might explain the increase in
470 relative abundance (Kartal et al., 2012). For NOB *Nitrospira*, except for formate usage,
471 there is to our knowledge no mixotrophic growth reported (Koch et al., 2015). The increase
472 in growth could thus be a consequence of certain auxotrophy and/or symbiosis, resulting in
473 a growth limitation when only glucose was fed. Because no batch activity test was executed
474 at the end of the experiment, the higher relative abundance could not be correlated with
475 an increase in sludge-specific activity, and further research will teach us if autotrophic
476 growth/activity can be boosted by introducing the right satellite community/substrate.

477 3.6 Microbial diversity steers reactor performance

478 The different operational conditions in the reactor steered the microbial community. The
479 community dynamics (β-diversity) NMDS plots show how the community changed over
480 time due to the operational changes. Overall, the floccular community was more impacted
481 by the changes in reactor conditions than the carrier. The most discriminating factor was
482 the bCOD type, where the change from glucose (bCOD/N 0.5-1) to a more complex bCOD
483 mixture (bCOD/N = 2) led to a completely different community in both the flocs and the
484 carrier (**Figure 3**). Furthermore, slight changes in aeration strategy and $AerSRT_{floc}$ also
485 changed the community and diversity. Lower $AerSRT_{floc}$ resulted in lower α-diversities in the
486 floc, which is in line with the findings of Meerburg et al. (2016) where a high-rate activated
487 sludge system had lower diversity than a low-rate activated sludge system.

488 The diversity changes that impacted the whole community were also noticed in the
489 autotrophic N-community (AnAOB, AerAOB, and NOB), with different AerAOB (OTU 98, 112
490 and 143) and NOB (*Nitrospira* lineage I vs lineage II) abundant at different timepoints
491 (**Figure 3, Panel 3 (NOB), and Figure 3, Panel 4 (AerAOB)**). For AerAOB and NOB, it is not
492 clear what conditions drove the community fluctuations between the different AerAOB
493 OTU and NOB lineage I and II. Since it is known for NOB *Nitrospira* that the potential activity
494 of lineage I is higher than lineage II, higher nitrite availability in the reactor might have
495 favored lineage I over lineage II (Nowka et al., 2015). Oxygen limitation on the other hand is
496 most likely not a discriminatory factor (Ushiki et al., 2017). Albeit, the microbial community
497 underwent considerable changes, in which each player will have had its own set of kinetics,
498 impacting the reactor performance and batch-test activities. Further work on which
499 AerAOB or NOB to select for, considering the impact of real pretreated sewage, might lead
500 towards optimal conditions to select the preferred microbial players for mainstream PN/A.

501 4 Conclusions

502 For a mainstream IFAS partial nitritation/anammox reactor, the best performance was
503 obtained at low $AerSRT_{floc}$ (~7d) and continuous aeration with two alternating DO
504 setpoints: 0.07-0.13 mg O_2 L^{-1} (10 min) and 0.27-0.43 mg O_2 L^{-1} (5 min). Under these
505 conditions, flocs acted as nitrite sources and carriers as nitrite sinks. Higher floccular sludge
506 concentration (~0.5-1 g VSS L^{-1}) allowed for sufficient aerobic ammonium conversion while
507 short $AerSRT_{floc}$ enabled higher floccular rAerAOB/rNOB. Lower DO setpoints (0.05 vs. 0.15
508 mg O_2 L^{-1}) resulted in higher carrier rAnAOB/rNOB. The next step towards practical
509 implementation is validation on real pretreated sewage and robustness tests.

510

511 E-supplementary data of this work can be found in online version of the paper.

512 5 Acknowledgements

513 D.S. was supported by a Ph.D. grant from the Institute for the Promotion of Innovation by
514 Science and Technology in Flanders (IWT-Vlaanderen, SB-131769). M.V.T. was supported by
515 a Ph.D. SB Fellowship from the Research Foundation - Flanders (FWO-Vlaanderen,
516 1S03218N).

517 6 References

518 1. Agrawal, S., Karst, S.M., Gilbert, E.M., Horn, H., Nielsen, P.H., Lackner, S. 2017. The role of
519 inoculum and reactor configuration for microbial community composition and dynamics in
520 mainstream partial nitritation anammox reactors. *Microbiologyopen*, **6**(4), 11.
521 2. Agrawal, S., Seuntjens, D., De Cocker, P., Lackner, S., Vlaeminck, S.E. 2018. Success of
522 mainstream partial nitritation/anammox demands integration of engineering, microbiome and
523 modeling insights. *Current Opinion in Biotechnology*, **50**, 214-221.
524 3. Dalsgaard, T., Stewart, F.J., Thamdrup, B., De Brabandere, L., Revsbech, N.P., Ulloa, O., Canfield,
525 D.E., DeLong, E.F. 2014. Oxygen at Nanomolar Levels Reversibly Suppresses Process Rates and
526 Gene Expression in Anammox and Denitrification in the Oxygen Minimum Zone off Northern
527 Chile. *Mbio*, **5**(6), 14.
528 4. De Clippeleir, H., Vlaeminck, S.E., De Wilde, F., Daeninck, K., Mosquera, M., Boeckx, P.,
529 Verstraete, W., Boon, N. 2013. One-stage partial nitritation/anammox at 15 A degrees C on
530 pretreated sewage: feasibility demonstration at lab-scale. *Applied Microbiology and*
531 *Biotechnology*, **97**(23), 10199-10210.
532 5. Du, R., Cao, S.B., Wang, S.Y., Niu, M., Peng, Y.Z. 2016. Performance of partial denitrification
533 (PD)-ANAMMOX process in simultaneously treating nitrate and low C/N domestic wastewater
534 at low temperature. *Bioresource Technology*, **219**, 420-429.
535 6. Edgar, R.C., Haas, B.J., Clemente, J.C., Quince, C., Knight, R. 2011. UCHIME improves sensitivity
536 and speed of chimera detection. *Bioinformatics*, **27**(16), 2194-2200.
537 7. Gilbert, E.M., Agrawal, S., Karst, S.M., Horn, H., Nielsen, P.H., Lackner, S. 2014. Low
538 Temperature Partial Nitritation/Anammox in a Moving Bed Biofilm Reactor Treating Low
539 Strength Wastewater. *Environmental Science & Technology*, **48**(15), 8784-8792.
540 8. Greenberg, A.E., Clesceri, L.S., Eaton, A.D. 1995. Standard methods for the examination of water
541 and wastewater. *American Public Health Association*.
542 9. Han, M., Vlaeminck, S.E., Al-Omari, A., Wett, B., Bott, C., Murthy, S., De Clippeleir, H. 2016.
543 Uncoupling the solids retention times of flocs and granules in mainstream deammonification: A

544 screen as effective out-selection tool for nitrite oxidizing bacteria. *Bioresource Technology*, **221**,
545 195-204.
546 10. Hubaux, N., Wells, G., Morgenroth, E. 2015. Impact of coexistence of flocs and biofilm on
547 performance of combined nitritation-anammox granular sludge reactors. *Water Research*, **68**,
548 127-139.
549 11. Kartal, B., de Almeida, N.M., Maalcke, W.J., Op den Camp, H.J.M., Jetten, M.S.M., Keltjens, J.T.
550 2013. How to make a living from anaerobic ammonium oxidation. *Fems Microbiology Reviews*,
551 **37**(3), 428-461.
552 12. Klindworth, A., Pruesse, E., Schweer, T., Peplies, J., Quast, C., Horn, M., Glockner, F.O. 2013.
553 Evaluation of general 16S ribosomal RNA gene PCR primers for classical and next-generation
554 sequencing-based diversity studies. *Nucleic Acids Research*, **41**(1), 11.
555 13. Koch, H., Lucker, S., Albertsen, M., Kitzinger, K., Herbold, C., Spieck, E., Nielsen, P.H., Wagner,
556 M., Daims, H. 2015. Expanded metabolic versatility of ubiquitous nitrite-oxidizing bacteria from
557 the genus Nitrospira. *Proceedings of the National Academy of Sciences of the United States of*
558 *America*, **112**(36), 11371-11376.
559 14. Lackner, S., Gilbert, E.M., Vlaeminck, S.E., Joss, A., Horn, H., van Loosdrecht, M.C.M. 2014. Full-
560 scale partial nitritation/anammox experiences - An application survey. *Water Research*, **55**, 292-
561 303.
562 15. Laureni, M., Falas, P., Robin, O., Wick, A., Weissbrodt, D.G., Nielsen, J.L., Ternes, T.A.,
563 Morgenroth, E., Joss, A. 2016. Mainstream partial nitritation and anammox: long-term process
564 stability and effluent quality at low temperatures. *Water Research*, **101**, 628-639.
565 16. Laureni, M., Weissbrodt, D.G., Villez, K., Robin, O. 2019. Biomass segregation between biofilm
566 and flocs improves the control of nitrite-oxidizing bacteria in mainstream partial nitritation and
567 anammox processes. *Water research*.
568 17. Lawson, C.E., Wu, S., Bhattacharjee, A.S., Hamilton, J.J., McMahon, K.D., Goel, R., Noguera, D.R.
569 2017. Metabolic network analysis reveals microbial community interactions in anammox
570 granules. *Nature Communications*, **8**, 12.
571 18. Le, T., Peng, B., Su, C., Massoudieh, A., Torrents, A., Al-Omari, A., Murthy, S., Wett, B.,
572 Chandran, K., deBarbadillo, C., Bott, C., De Clippeleir, H. 2019. Nitrate residual as a key
573 parameter to efficiently control partial denitrification coupling with anammox. *Water*
574 *Environment Fedaration*.
575 19. Li, J.L., Zhang, L., Peng, Y.Z., Yang, S.H., Wang, X.L., Li, X.Y., Zhang, Q. 2019. NOB suppression in
576 partial nitritation-anammox (PNA) process by discharging aged flocs: Performance and
577 microbial community dynamics. *Chemosphere*, **227**, 26-33.
578 20. Lotti, T., Kleerebezem, R., Hu, Z., Kartal, B., de Kreuk, M.K., Kip, C.V.T., Kruit, J., Hendrickx,
579 T.L.G., van Loosdrecht, M.C.M. 2015. Pilot-scale evaluation of anammox-based mainstream
580 nitrogen removal from municipal wastewater. *Environmental Technology*, **36**(9), 1167-1177.
581 21. Lowry, O.H., Rosebrough, N., Farr, A.L., Randall, R.J. 1951. Protein measurement with the Folin
582 phenol reagent. *Journal of biological Chemistry*.
583 22. Malovanyy, A., Trela, J., Plaza, E. 2015. Mainstream wastewater treatment in integrated fixed
584 film activated sludge (IFAS) reactor by partial nitritation/anammox process. *Bioresource*
585 *Technology*, **198**, 478-487.
586 23. McMurdie, P.J., Holmes, S. 2014. Waste not, want not: why rarefying microbiome data is
587 inadmissible. *PLoS computational biology*.
588 24. Meerburg, F.A., Vlaeminck, S.E., Roume, H., Seuntjens, D., Pieper, D.H., Jauregui, R., Vilchez-
589 Vargas, R., Boon, N. 2016. High-rate activated sludge communities have a distinctly different
590 structure compared to low-rate sludge communities, and are less sensitive towards
591 environmental and operational variables. *Water Research*, **100**, 137-145.

25. Nielsen, M., Bollmann, A., Sliekers, O., Jetten, M., Schmid, M., Strous, M., Schmidt, I., Larsen, L.H., Nielsen, L.P., Revsbech, N.P. 2005. Kinetics, diffusional limitation and microscale distribution of chemistry and organisms in a CANON reactor. *Fems Microbiology Ecology*, **51**(2), 247-256.
26. Nowka, B., Daims, H., Spieck, E. 2015. Comparison of Oxidation Kinetics of Nitrite-Oxidizing Bacteria: Nitrite Availability as a Key Factor in Niche Differentiation. *Applied and Environmental Microbiology*, **81**(2), 745-753.
27. Pedrouso, A., Trela, J., Val del Rio, A., Mosquera-Corral, A., Plaza, E. 2019. Performance of partial nitritation-anammox processes at mainstream conditions in an IFAS system. *Journal of environmental Management*.
28. Props, R., Monsieurs, P., Mysara, M., Clement, L., Boon, N. 2016. Measuring the biodiversity of microbial communities by flow cytometry. *Methods in Ecology and Evolution*, **7**(11), 1376-1385.
29. Regmi, P., Miller, M.W., Holgate, B., Bunce, R., Park, H., Chandran, K., Wett, B., Murthy, S., Bott, C.B. 2014. Control of aeration, aerobic SRT and COD input for mainstream nitritation/denitritation. *Water Research*, **57**, 162-171.
30. Schloss, P.D., Westcott, S.L., Ryabin, T., Hall, J.R., Hartmann, M., Hollister, E.B., Lesniewski, R.A., Oakley, B.B., Parks, D.H., Robinson, C.J., Sahl, J.W., Stres, B., Thallinger, G.G., Van Horn, D.J., Weber, C.F. 2009. Introducing mothur: Open-Source, Platform-Independent, Community-Supported Software for Describing and Comparing Microbial Communities. *Applied and Environmental Microbiology*, **75**(23), 7537-7541.
31. Seuntjens, D., Carvajal-Arroyo, J.M., Ruopp, M., Bunse, P., De Mulder, C.P., Lochmatter, S., Agrawal, S., Boon, N., Lackner, S., Vlaeminck, S.E. 2018a. High-resolution mapping and modeling of anammox recovery from recurrent oxygen exposure. *Water Research*, **144**, 522-531.
32. Seuntjens, D., Van Tendeloo, M., Chatzigiannidou, I., Carvajal-Arroyo, J.M., Vandendriessche, S., Vlaeminck, S.E., Boon, N. 2018b. Synergistic Exposure of Return-Sludge to Anaerobic Starvation, Sulfide, and Free Ammonia to Suppress Nitrite Oxidizing Bacteria. *Environmental Science & Technology*, **52**(15), 8725-8732.
33. Speth, D.R., in 't Zandt, M.H., Guerrero-Cruz, S., Dutilh, B.E., Jetten, M.S.M. 2016. Genome-based microbial ecology of anammox granules in a full-scale wastewater treatment system. *Nature Communications*, **7**, 10.
34. Srinandan, C.S., Shah, M., Patel, B., Nerurkar, A.S. 2011. Assessment of denitrifying bacterial composition in activated sludge. *Bioresource Technology*, **102**(20), 9481-9489.
35. Third, K.A., Sliekers, A.O., Kuenen, J.G., Jetten, M.S.M. 2001. The CANON system (completely autotrophic nitrogen-removal over nitrite) under ammonium limitation: Interaction and competition between three groups of bacteria. *Systematic and Applied Microbiology*, **24**(4), 588-596.
36. Ushiki, N., Jinno, M., Fujitani, H., Suenaga, T., Terada, A., Tsuneda, S. 2017. Nitrite oxidation kinetics of two Nitrospira strains: The quest for competition and ecological niche differentiation. *Journal of Bioscience and Bioengineering*, **123**(5), 581-589.
37. van de Graaf, A.A., de Bruijn, P., Robertson, L.A., Jetten, M.S.M., Kuenen, J.G. 1996. Autotrophic growth of anaerobic ammonium-oxidizing micro-organisms in a fluidized bed reactor. *Microbiology-Uk*, **142**, 2187-2196.
38. Vilchez-Vargas, R., Geffers, R., Suarez-Diez, M., Conte, I., Waliczek, A., Kaser, V.S., Kralova, M., Junca, H., Pieper, D.H. 2013. Analysis of the microbial gene landscape and transcriptome for aromatic pollutants and alkane degradation using a novel internally calibrated microarray system. *Environmental Microbiology*, **15**(4), 1016-1039.
39. Vlaeminck, S.E., Terada, A., Smets, B.F., De Clippeleir, H., Schaubroeck, T., Bolca, S., Demeestere, L., Mast, J., Boon, N., Carballa, M., Verstraete, W. 2010. Aggregate Size and

Architecture Determine Microbial Activity Balance for One-Stage Partial Nitritation and Anammox. *Applied and Environmental Microbiology*, **76**(3), 900-909.

40. Wiesmann, U. 1994. Biological nitreogen removal from wastewater. *Biotechnics/wastewater*, **51**, 113-154.
41. Winkler, M.K.H., Bassin, J.P., Kleerebezem, R., Sorokin, D.Y., van Loosdrecht, M.C.M. 2012. Unravelling the reasons for disproportion in the ratio of AOB and NOB in aerobic granular sludge. *Applied Microbiology and Biotechnology*, **94**(6), 1657-1666.
42. Yang, Y.D., Zhang, L., Cheng, J., Zhang, S.J., Li, B.K., Peng, Y.Z. 2017. Achieve efficient nitrogen removal from real sewage in a plug-flow integrated fixed-film activated sludge (IFAS) reactor via partial nitritation/anammox pathway. *Bioresource Technology*, **239**, 294-301.

7 Figure Captions

Table 1 Operational phases with their performance data, chosen at stable operational conditions during the 'calculation period (d)'. For bCOD/N = 0.25-1, the used carbon source was glucose. [+] For bCOD/N = 2, the mixture consisted of acetate (20%), starch (65%) and yeast extract (15%, about 1 mg N L^{-1}) to represent the more slowly biodegradable nature of bCOD in aerobically pretreated sewage. **Values in bold** highlight the changes between the different operational periods. *For two-point continuous aeration: low DO setpoint (10 min); high DO setpoint (5 min).

Figure 1 Depicting the relationship between operational conditions (Panel A-C) and reactor performance (Panel D). Main variables: floccular aerobic sludge retention time ($AerSRT_{floc}$) (Panel A) and aeration strategy (Panel B). Side variables (Panel C): N-loading rate and influent bCOD/N ratio. Gey shaded area corresponds to the ideal range of $AerSRT_{floc}$ during best performing Phase VIa. Yellow shaded area indicates higher aeration setpoints, while the red shaded area indicates a period of difficult $AerSRT_{floc}$ control. Nitrate production ratio: produced nitrate on converted ammonium - produced nitrite

Figure 2 Activity distribution between flocs and carriers for AnAOB, AerAOB and NOB as derived from the potential activities obtained in the batch tests, fitted to the reactor

667 performance of the different phases (**M&M Section 2.4**). In the left top corner, the legend
668 is shown. Different operational phases; Phase I (lowest NOB suppression), Phase IV & Phase
669 V (intermediate NOB suppression), and Phase IIb & Phase VIa (highest NOB suppression).
670 With X-floc: floccular sludge concentration.

671 **Figure 3** Telezoom on the impact of different operational parameters **1)** on the microbial
672 community for flocs and carriers. Zoom in starts from **2)** relative abundance of the 15 most
673 abundant phyla in the total community, towards **3)** relative abundance of the most
674 abundant AerAOB, AnAOB and NOB genera and species of the autotrophic N-community
675 and **4)** relative abundance within the *Nitrosomonas* community. Data shown is a triplicate
676 for floc/carrier at each timepoint.. Shaded areas in the table highlight areas of interest to
677 compare the different timepoints. The big black arrow indicates an inoculation timepoint.
678 At day 213 and day 325 no samples of carrier or flocs were taken, respectively. *At these
679 timepoints, batch activity tests were executed. ⁺Aeration strategy: continuous aeration:
680 one-point; or two-point aeration: 10 min. low setpoint; 5 min. high setpoint.

681 **Figure 4** Relationship between carrier rAnAOB/rNOB, as measured in batch tests, and
682 nitrate production ratio (%) in the reactor. For each data-point, the $AerSRT_{floc}$ is depicted as
683 the blue shaded area.

684 **Figure 5** Impact of bCOD spikes on reactor performance at day 288. The spikes were given
685 after the 45 minutes feeding phase ended. bCOD spikes consisted of acetate (20%), yeast
686 extract (15%) and starch (65%), and were given under a low (0.05 mg O_2 L^{-1}; first spike) and
687 high (0.3 mg O_2 L^{-1}; second spike) DO-setpoint.

8 Tables and Figures

Dries Seuntjens: Conceptualization, Methodology, Investigation, Visualization, Writing – Original Draft; **Jose M. Carvajal Arroyo**: Conceptualization, Supervision; **Michiel Van Tendeloo**: Visualization, Writing – Original Draft; **Ioanna Chatzigiannidou**: Methodology, Software; **Janet Molina**: Investigation; **Samnang Nop**: Software; **Nico Boon**: Writing – Reviewing and Editing; **Siegfried E. Vlaeminck**: Writing – Reviewing and Editing

Declaration of interests

☒ The authors declare that they have no known competing financial interests or personal relationships that could have appeared to influence the work reported in this paper.

☐The authors declare the following financial interests/personal relationships which may be considered as potential competing interests:

706

707

708

	Phase (days)	DO (mg O_2 L^{-1})	$AerSRT_{floc}$ (d)	Influent bCOD/N (-)	N loading rate (mg N $L^{-1}d^{-1}$)	N removal rate (mg N $L^{-1}d^{-1}$)	N removal (%)	Nitrate production ratio (%)	Operation time (x times $AerSRT_{floc}$)	Calculation period (d) (n measurements)
One-point aeration	**I (0-44)**	0.15±0.03	26.1±8.4	0.25	152±34	40±8	25±5	71±8	1.7	0 - 44 (24)
	IIa (45-59)	**0.06±0.01**	**8.2±5**	0.25	150±17	14±5	10±3	65±16	1.7	45 - 59 (15)
	IIb (61-73)	0.06±0.01	7.7±5	0.25	**61±6**	8±3	14±4	33±9	1.7	61 - 73 (10)
	III (109-123)	**0.15±0.03**	7.5±2.7	0.5	59±9	9±4	14±5	80±9	1.9	109 - 123 (11)
	IV (124-164)	0.15±0.02	**4.9±1**	0.5	65±3	21±2	31±3	38±4	8.2	136 - 150 (11)
Two-point aeration*	**V (165-212)**	**0.10; 0.27**	4.1±0.8	0.5	64±2	20±4	30±5	44±7	11.6	165 - 212 (13)
	VIa (213-246)	0.07; 0.31	**6.8±3**	**0.5-1**	**153±10**	122±23	73±13	18±6	6.4	239 - 256 (12)
	(247-256)	0.13; 0.47								
	VIb (257-268)	0.13; 0.47	**5.5±1.8**	**2⁺**	179±23	131±29	68±9	22±8	5.5	259 - 287 (19)
	(269-325)	0.05; 0.32								

709

710

711

712 • Integrated fixed-film activated sludge tested for shortcut nitrogen removal
713 • Combining strategies selectively suppressed activity nitrite oxidizing bacteria
714 • Flocs acted as nitrite source, while carriers were nitrite sinks
715 • Optimal nitrite source: low, but sufficient aerobic floc retention time (±7 days)
716 • Optimal sink: dissolved oxygen <0.47 mg O_2 L^{-1} and N loading rate >150 mg N L^{-1} d^{-1}

717